ACADEMIC PRESS

Available online at www.sciencedirect.com
SCIENCE DIRECT®

NeuroImage

NeuroImage 19 (2003) 577–586

www.elsevier.com/locate/ynimg

# Physiological self-regulation of regional brain activity using real-time functional magnetic resonance imaging (fMRI): methodology and exemplary data

Nikolaus Weiskopf,[a,b,*] Ralf Veit,[a] Michael Erb,[b] Klaus Mathiak,[b,c] Wolfgang Grodd,[b] Rainer Goebel,[d] and Niels Birbaumer[a,e]

[a] *Institute of Medical Psychology and Behavioural Neurobiology, University of Tübingen, Tübingen, Germany*
[b] *Section of Experimental MR of the CNS, Department of Neuroradiology, University of Tübingen, Tübingen, Germany*
[c] *Department of Neurology, University of Tübingen, Tübingen, Germany*
[d] *Department of Cognitive Neuroscience, Faculty of Psychology, University of Maastricht, Maastricht, The Netherlands*
[e] *Center for Cognitive Neuroscience, University of Trento, Trento, Italy*

Received 15 July 2002; revised 11 February 2003; accepted 14 February 2003

**Abstract**

A brain–computer interface (BCI) based on real-time functional magnetic resonance imaging (fMRI) is presented which allows human subjects to observe and control changes of their own blood oxygen level-dependent (BOLD) response. This BCI performs data preprocessing (including linear trend removal, 3D motion correction) and statistical analysis on-line. Local BOLD signals are continuously fed back to the subject in the magnetic resonance scanner with a delay of less than 2 s from image acquisition. The mean signal of a region of interest is plotted as a time-series superimposed on color-coded stripes which indicate the task, i.e., to increase or decrease the BOLD signal. We exemplify the presented BCI with one volunteer intending to control the signal of the rostral–ventral and dorsal part of the anterior cingulate cortex (ACC). The subject achieved significant changes of local BOLD responses as revealed by region of interest analysis and statistical parametric maps. The percent signal change increased across fMRI-feedback sessions suggesting a learning effect with training. This methodology of fMRI-feedback can assess voluntary control of circumscribed brain areas. As a further extension, behavioral effects of local self-regulation become accessible as a new field of research.
© 2003 Elsevier Science (USA). All rights reserved.

*Keywords:* Self-regulation; Physiological regulation; Real-time functional magnetic resonance imaging; Brain–computer interface; fMRI-feedback; Feedback; Neurofeedback; Blood oxygen level-dependent; Anterior cingulate

## Introduction

Voluntary regulation of electrical brain activity can be achieved by on-line feedback training of a particular component of the electroencephalogram (EEG; Birbaumer et al., 1990). Physiological self-regulation of electrical brain activity produces specific behavioral effects dependent upon the functional role of the regulated brain area; for instance, voluntary regulation of sensorimotor areas increased tactile sensitivity or decreased reaction time in a motor task locally for one hemisphere (Birbaumer et al., 1990; Rockstroh et al., 1990). Feedback training of slow cortical potentials was used to suppress seizures in intractable epilepsy (Kotchoubey et al., 2001) and to enable paralyzed patients to communicate via brain potentials by selecting letters and words using a brain–computer interface (BCI; Birbaumer et al., 1999).

There is increasing evidence for a strong correlation between the blood oxygen level-dependent (BOLD) signal measured by functional magnetic resonance imaging (fMRI) and electric brain activity, in particular local field

* Corresponding author. University of Tübingen, MEG-Center, Institute of Medical Psychology and Behavioural Neurobiology, Otfried-Müller-Str. 47, 72076 Tübingen, Germany. Fax: +49-7071-295706.
*E-mail address:* nikolaus.weiskopf@uni-tuebingen.de (N. Weiskopf).

1053-8119/03/$ – see front matter © 2003 Elsevier Science (USA). All rights reserved.
doi:10.1016/S1053-8119(03)00145-9

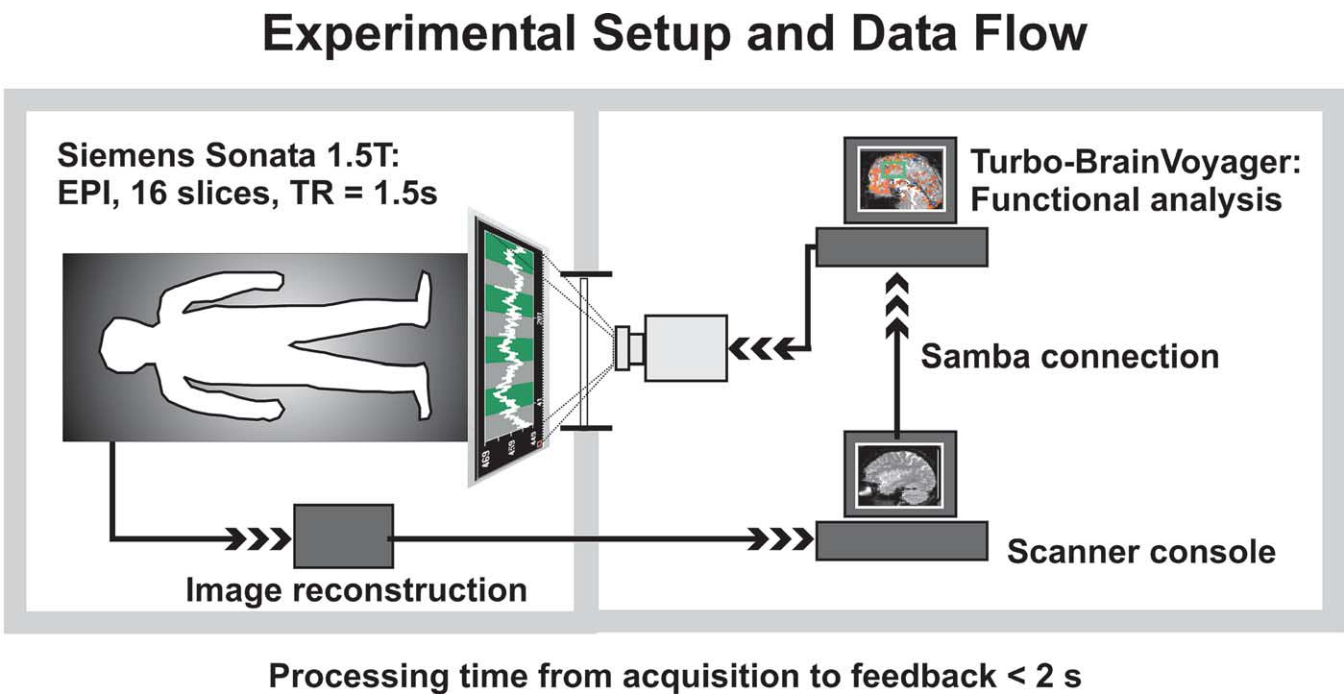


Fig. 1. Setup of the fMRI brain–computer interface. Images are acquired and reconstructed on-line by the clinical MRI system (1.5 T, Siemens Magnetom Sonata). Turbo-Brain Voyager (Goebel, 2001) performs statistical analysis and visualization on a separate personal computer, which retrieves the images from the scanner console via a Samba connection (Eckstein et al., 1999) as soon as they are reconstructed. Data transfer, preprocessing (including linear trend removal and 3D motion correction), statistical analysis, and display of feedback are performed on-line with a delay of less than 2 s with respect to image acquisition.

potentials (e.g., Logothetis et al., 2001; Arthurs and Boniface, 2002). Moreover, studies combining fMRI with EEG showed correlations between the amplitude and localization of the electric generators and localized BOLD signal changes (e.g., Ball et al., 1999; Arthurs et al., 2000).

During recent years, fMRI data acquisition and processing techniques have improved considerably. Increased image-encoding gradient power and higher magnetic field strength allow for fast image encoding with an adequate signal-to-noise ratio (SNR). In addition, faster computers and data processing software can reconstruct images and perform statistical analysis in real-time, e.g., recursive correlation analysis (Cox et al., 1995), parallelized on-line analysis (Goddard et al., 1997), functional scout using MR receiver phase cycling (Goodyear et al., 1997), intraoperative real-time fMRI (Gering and Weber, 1998), real-time paradigm control (Voyvodic, 1999), on-line motion correction (Cox and Jesmanowicz, 1999), increased BOLD sensitivity by reference vector optimization (Gembris et al., 2000), cortex-based analysis and visualization (Goebel, 2001), robust on-line motion correction (Mathiak and Posse, 2001), single-event related real-time fMRI (Posse et al., 2001), and real-time multiple linear regression (Smyser et al., 2001).

Encouraged by the progress in real-time data processing and the new knowledge on the coupling of neuroelectric and BOLD signals, we aimed at transferring the concept of on-line feedback of electric brain signals to BOLD signals, because the high spatial resolution of fMRI could be used to provide feedback of circumscribed brain regions.

Two recent studies applied different types of delayed feedback (by approx. 60 s) of fMRI signals. One study suggests that visual feedback of functional brain activation maps can guide subjects to adjust their motor behavior in order to expand activation in the motor and somatosensory cortex (Yoo and Jolesz, 2002). The other study provided the subjects with feedback of the BOLD signal change in the amygdala–hippocampal area based on the experimenter's rating following a negative mood induction task combined with presentation of neutral and sad faces (Posse et al., 2003). Effects related to the visual presentation of facial expressions could not be separated from the effects of the feedback. In comparison with these studies, the present methodological study emphasized the immediate feedback of local BOLD signals, because previous studies on feedback of EEG (Mulholland et al., 1979; Rockstroh et al., 1990) indicated that minimum delays between response and feedback facilitate self-regulation.

To this end, a fMRI-BCI was developed which allows human subjects to observe the changes of the BOLD signal in specific brain regions in real-time with a delay of less than 2 s from the acquisition of the magnetic resonance image. To exemplify the feasibility of on-line feedback and physiological regulation of the BOLD signal, one healthy subject was trained to increase and decrease the BOLD signal of the anterior cingulate cortex (ACC). From ana-

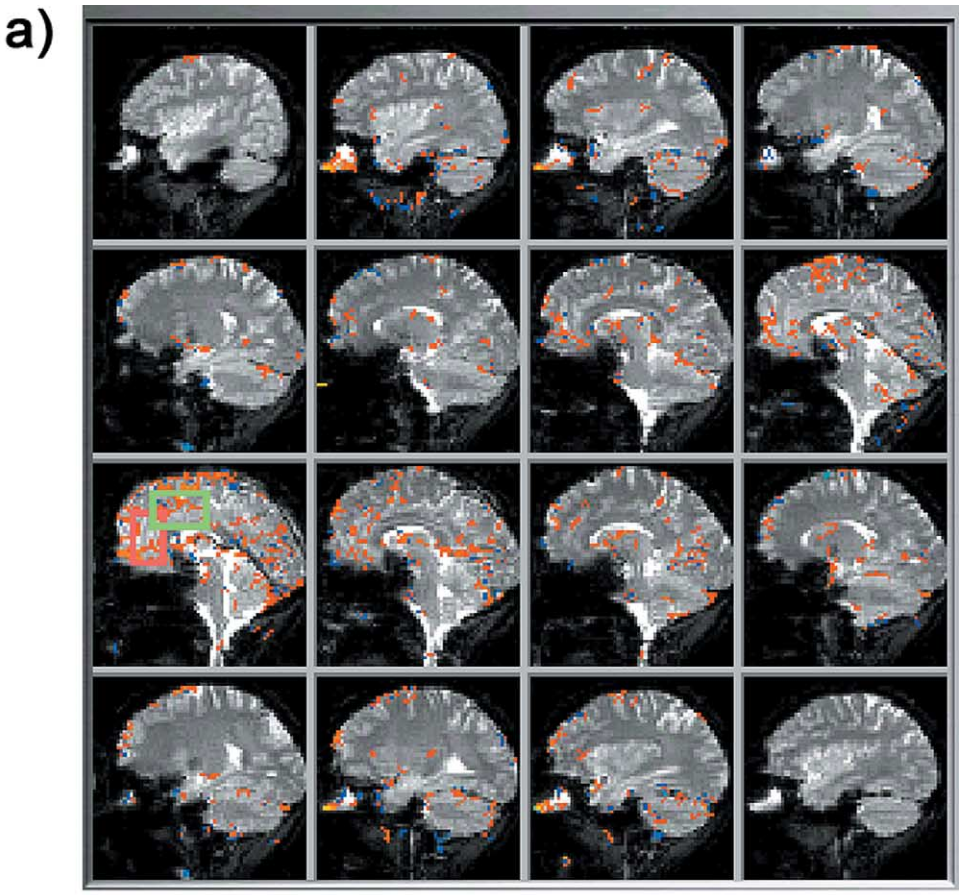
a)
b)
Activation = Increase Signal
Baseline = Return to Baseline
Average Signal Intensity
469
459
449
41
201
Rostral-Ventral ACC
Average Signal Intensity
460
450
440
41
201
Dorsal ACC
Amplitude (mm/deg)
1
0
-1
41
201
Head Motion
60 s
300 s
Number of Volumes / Time

tomical and neuroimaging studies two major subdivisions of the ACC can be distinguished, which possibly subserve distinct functions: the dorsal "cognitive" division (ACcd) and the rostral–ventral "affective" division (ACad; Bush et al., 2000). Due to their involvement in different functional neural networks, physiological self-regulation could be applied to study cognitive and emotional parameters, e.g., emotional valence or arousal, dependent upon differential activation of the two subdivisions. We presented discrete feedback of ACcd and ACad to the volunteer in order to assess the possibility to control the BOLD-response of these brain areas. Additionally, effects of self-regulation of the BOLD-response on subjective feelings of valence (pleasentness) and arousal during feedback training were studied. Previous imaging work has identified a correlation between arousal and the BOLD signal in the ACC (e.g., Paus, 2001; Critchley et al., 2001).

## Overview of the method

To obtain exemplary data, one healthy right-handed subject (male, age 28) was trained to voluntarily control the local BOLD signal of the anterior cingulate cortex (ACC) using the fMRI brain–computer interface. Informed written consent was obtained prior to the study in accordance with the local ethics committee.

### *fMRI data acquisition and on-line data processing*

The fMRI brain–computer interface (BCI) used for feedback of regional BOLD signals was based on Turbo-BrainVoyager (Brain Innovation, Maastricht, The Netherlands; Goebel, 2001) and a 1.5 T whole body scanner with standard head coil (Magnetom Sonata, Siemens, Erlangen, Germany). After on-line reconstruction by the scanner hardware, the images were stored in mosaic file format (Klose et al., 1999). File names were numbered in ascending order and accessed via a Samba connection (Eckstein et al., 1999) by a personal computer with Windows 98 SE operating system (Microsoft Corporation, Redmond, WA, USA). On this computer, Turbo-BrainVoyager retrieved the files according to their numbering as soon as they were created by the image reconstruction system. It performed data preprocessing, statistical analysis, and BOLD signal feedback in real-time. Fig. 1 illustrates the technical setup and data flow.

Preprocessing of the data included incremental linear detrending of the time-series and 3D motion correction, i.e., all subsequent functional imaging volumes were realigned to the first recorded volume as they became available during the scan using a rigid body transformation. Correlation analysis was performed cumulatively using the recursive least squares regression algorithm (Pollock, 1999). Linear detrending was implemented by adding a linear predictor as a confound to the general linear model (GLM). To visualize the fMRI data, incrementally updated correlation maps were presented (Fig. 2a) and the average signals of two box-shaped regions of interest (ROI)—each encompassing one subdivision of the anterior cingulate cortex (ACC)—were plotted as time courses superimposed over the color-coded background indicating the task (Fig. 2b). Head motion was determined on-line and presented to the subject in order to alleviate the control of head movements.

As a trade-off between adequate spatial coverage, high BOLD contrast by using an optimum echo time (Gati et al., 2000), and imaging speed, 16 parasagittal slices were acquired using an echo-planar imaging sequence (EPI; repetition time TR = 1.5 s, matrix size = 64 × 64, voxel size = 3.75 × 3.75 × 4 $mm^3$, reduced to 3 × 3 × 4 $mm^3$ for sessions 4–8, slice gap = 1 mm, effective echo time TE = 45 ms, flip angle $\alpha = 70°$, bandwidth = 1.3 kHz/pixel). The first five volumes of each session were excluded from statistical analysis to account for T1 equilibration effects. The subject was in supine position on the padded scanner couch and wearing hearing protection with built-in headphones. In order to reduce movements, the participant's head was padded with two foam cushions at both sides. The volunteer was a member of the laboratory, experienced in participation in fMRI studies, and was aware of the necessity to avoid moving any parts of the body, in particular the head. For superposition of functional activations over anatomical details, a high resolution T1-weighted structural scan of the whole brain was obtained (FLASH 3D, matrix size = 256 × 256, 176 partitions, 1 $mm^3$ isotropic voxels, TR = 14 ms, TE = 5.6 ms, $\alpha = 25°$).

### *Feedback task*

During feedback sessions, the average BOLD signals from two regions of interest (ROI) encompassing the rostral–ventral (ACad) and dorsal (ACcd) ACC were presented to the subject by video projection (visual field 7° × 10° at 1.2 m distance). Monitoring the continuously updated time-series (Fig. 2b), the subject should control the regional BOLD signals in two different conditions. During activation

Fig. 2. Displays of real-time analysis software. (a) Correlation maps were superimposed over the sagittal EPI images and updated continuously within 2 s after image acquisition. In the median slice, the selected regions of interest (ROI) encompassed the dorsal (green box) and the adjacent rostral–ventral (red box) subdivision of the anterior cingulate cortex (ACC). (b) Upper two panels: the paradigm was presented by grey (baseline) and green stripes (activation, i.e., signal increase) with the BOLD signal time course superimposed (white curve; upper panel: rostral–ventral ACC, middle panel: dorsal ACC). Increase of BOLD signal moved the white curve upward during activation blocks. Lower panel: head motions were detected and corrected. Six motion parameters (translation in mm and rotation in degrees) were displayed on-line.

blocks he had to increase the BOLD signals, i.e., raise the signal curves, and during baseline blocks he had to decrease the BOLD signal, i.e., return the signal curves to the pretask level. To inform the subject about the current task, the two different types of blocks were presented as stripes of two different colors (Fig. 2b). These stripes served as background of the BOLD signal time-series. Each activation block (60 s) was preceded by a baseline block (60 s). Each feedback session comprised four pairs of activation and baseline blocks. The subject participated in two experiments comprising three and five sessions, respectively.

An established non–verbal pictorial technique (Bradley and Lang, 1994) assessed the affective state after each session; separately for activation and baseline blocks, the participant rated his affective state on two scales representing emotional valence and arousal. The scales ranged from 1 (negative valence/low arousal) to 9 (positive valence/high arousal).

The participant was not instructed to use a particular strategy to control the BOLD signal, but reported the mental strategy he had used after the fMRI experiment.

### *Off-line data analysis*

In addition to the on-line data processing, off-line ROI analysis of ACcd and ACad was performed in order to quantify the amount of voluntary control of the BOLD signal. Moreover, statistical parametric mapping across the entire volume assessed the neural correlate of physiological self-regulation and determined the anatomical specificity of the BOLD-response.

Employing the fMRI analysis package SPM99 (Wellcome Department of Cognitive Neurology, Queens Square, London, UK), EPI scans were corrected for motion and coregistered to the T1-weighted structural image (Friston et al., 1995). This structural image was spatially normalized to an anatomical template and the same nonlinear transformation was applied to the EPI images which were resampled with a voxel size of $2 \times 2 \times 2$ mm$^3$ (Ashburner and Friston, 1999). The anatomical template provided by the Montreal Neurologic Institute (MNI template; Collins et al., 1994) can be transformed (Brett et al., 2001) into the stereotaxic space described in the atlas of Talairach and Tournoux (Nowinski et al., 1997). After normalization, EPI images were spatially smoothed using a Gaussian kernel with 10 mm full width at half maximum (FWHM) to condition for random field theory which was applied to correct for multiple comparisons in statistical parametric mapping (Worsley and Friston, 1995).

To account for drifts and autocorrelations of the fMRI signal, the time-series of each voxel was high-pass (cut off period set to twice the duration of the activation and baseline block) and low-pass filtered (Gaussian, FWHM = 4 s). A general linear model (GLM) was applied to the time-course of each voxel (Worsley and Friston, 1995). A box-car reference function modeled the activation blocks. To account for neurovascular coupling and its delay with respect to neural activity, the reference function was convolved with a canonical hemodynamic response function (bi-gamma function with 6 s peak-delay) and its time derivative. In order to suppress artifacts caused by head motion, covariates derived from motion parameters (six per scan) were included into the GLM (Friston et al., 1996). They consisted of movement estimates obtained at the time of the current scan and the previous scan and their squared values ($4 \times 6 = 24$ covariates).

Statistical parametric maps reflected the signal increase and decrease during activation as compared to baseline blocks for each session separately. This analysis allowed to explore the data for potential learning effects, i.e., increases of signal change across sessions. The average change in brain activity across all sessions was analyzed using a fixed effect analysis. Statistical inference was based on the resulting $t$ statistics for each voxel and corrected for multiple comparisons by applying the theory of random Gaussian fields (Worsley et al., 1996). Activation clusters exceeding a spatial extent of 100 voxels (0.8 ml) at a voxel-wise threshold of $P < 0.05$ (volume-corrected) were considered significant.

Quantitative analysis was based on two regions of interest (Devinsky et al., 1995; Bush et al., 2000): the rostral–ventral part of the ACC (ACad) and the dorsal part of the ACC (ACcd). The ACad was defined as the rostral–ventral part of the ACC anterior to the vertical plane through Talairach coordinate $Y = 30$ mm resembling Brodmann Areas (BA) 25 and 33, as well as rostral BA 24 and 32. The ACcd was defined as the remaining part of the ACC, consisting of ACC superior to the corpus callosum between the vertical plane $Y = 30$ mm and $Y = 0$ mm. According to refined cytoarchitectonic specifications by Vogt et al. (1995), it included BA 24′ and 32′ (Fig. 3). Each ROI was marked on the normalized individual anatomical scan using the image viewing tool MRIcro (Rorden and Brett, 2000).

Mean signal intensities of the ROIs were determined for each functional image. The same GLM and preprocessing used for statistical parametric mapping were applied to the extracted ROI time-series. The percent signal change during activation as compared to baseline blocks was tested for significant increase during activation blocks employing a $t$ test. Moreover, to control for global signal changes correlated with the feedback task, the time-series of the average signal intensity across the entire imaging volume was statistically analyzed the same way as the ROI time-series.

Learning effects were assessed by testing whether the achieved BOLD-response increased with feedback training; sessions were numbered consecutively from 1 to 8, and the session numbers were correlated with the percent signal changes of the sessions (Spearman-Rho, one-sided).

To assess behavioral effects of the training, self-rated emotional valence and arousal were tested for a difference between activation blocks and baseline blocks using two-sided Wilcoxon signed rank tests. In addition, changes of

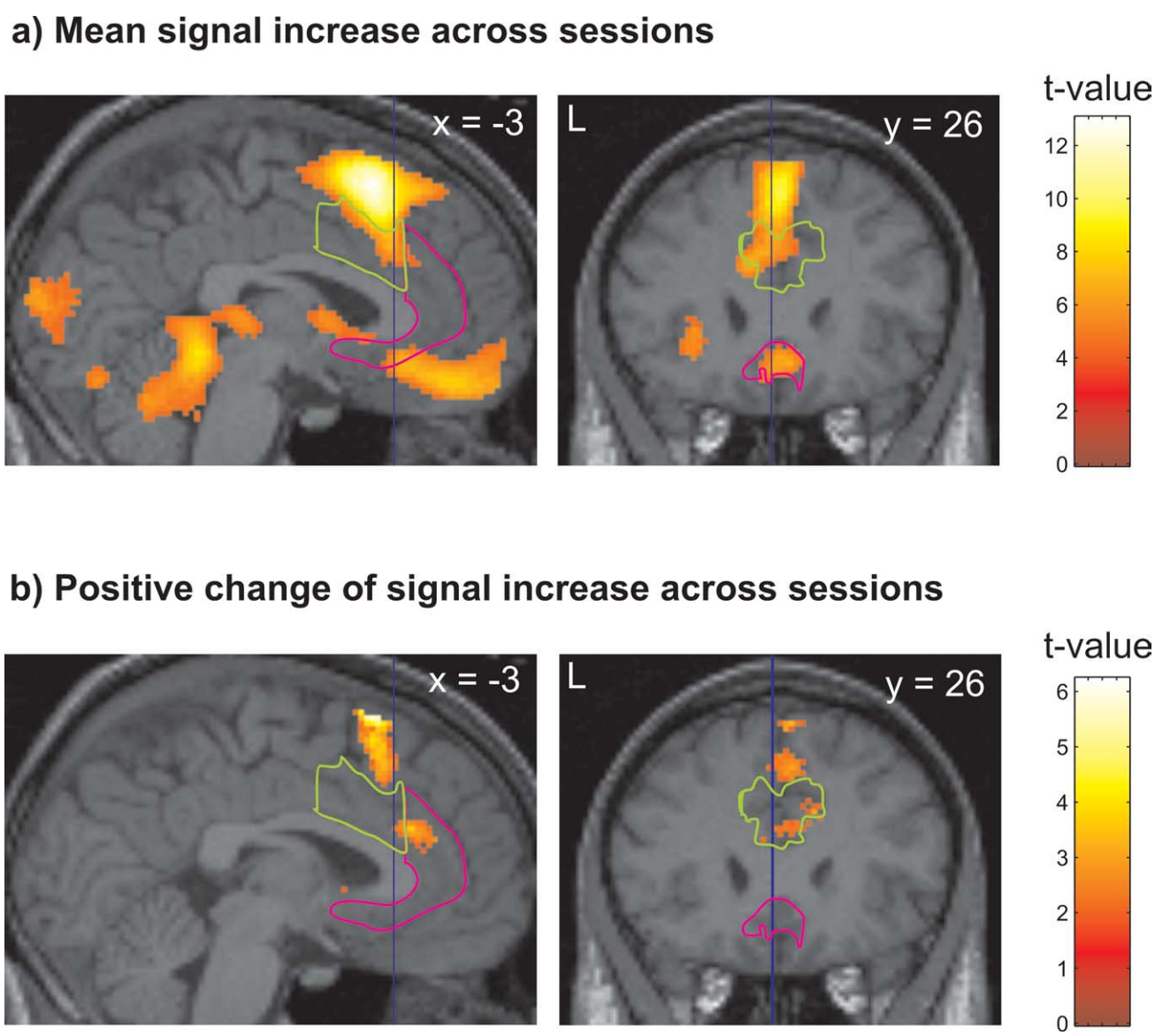


Fig. 3. Off-line statistical parametric mapping. (a) Signal increases during activation blocks are superimposed over individual normalized T1-weighted 3D MRI (MNI stereotaxic space; Collins et al., 1994) and thresholded at a significance level $P < 0.05$ (volume-corrected) with minimum spatial extent of 10 voxels. The region of interest analysis was performed on the rostral–ventral subdivision (ACad, borders marked in magenta), and dorsal subdivision (ACcd, borders marked in green) of the anterior cingulate cortex (ACC). Signal increases were observed in rostral–ventral and dorsal ACC during activation blocks. There were also activations in supplementary motor area (SMA), gyrus rectus, cerebellum, and calcarine fissure. (b) An increase of signal change across feedback sessions emerged at the rostral–ventral ACC, the SMA, and basal ganglia as revealed by post hoc analysis (corrected $P < 0.01$, voxel and cluster level) and indicated a possible learning effect (see also Fig. 4).

behavioral measures were correlated with signal changes per session detected within the ROIs using Spearman-Rho (two-sided). Statistical analysis was conducted with SPSS 10.0.7 (SPSS Inc., Chicago, IL, USA). Test values exceeding a threshold of $P < 0.05$ were considered to be significant.

### Summary of the materials and equipment

1. Data acquisition
   - fMRI: 1.5 T whole body scanner (Magnetom Sonata, Siemens, Erlangen, Germany)
   - Affective state: self-assessment manikin by Bradley and Lang (1994)
2. On-line data analysis
   - Data preprocessing and statistical analysis: Turbo-BrainVoyager (Brain Innovation, Maastricht, The Netherlands; Goebel, 2001) on a personal computer (RAM 768 MBytes; Dual Pentium III 866 MHz, Intel Corporation, Santa Clara, CA, USA) with Windows 98 SE operating system (Microsoft Corporation, Redmond, WA, USA)
   - Data transfer: Samba connection (Eckstein et al.,

1999) between scanner hardware with Solaris 1 operating system (SunOS Release 4.1.4, Sun Microsystems, Santa Clara, CA, USA) and the personal computer

3. Off-line data analysis
   - Statistical parametric mapping: SPM99 (Wellcome Department of Cognitive Neurology, Queens Square, London, UK), KULeuven automation tools (MR Research Center, Department of Radiology, University Hospitals Leuven, Belgium)
   - ROI analysis: SPM99, MRIcro (Rorden and Brett, 2000), and custom-made tools based on Matlab 5.3 (The MathWorks, Natick, MA, USA)
   - Behavioral and ROI data: SPSS 10.0.7 (SPSS Inc., Chicago, IL, USA)

## Results: exemplary single subject data

### *Behavioral data*

The subject rated the valence of his affective state significantly more positive for activation blocks as compared to baseline blocks (score for activation vs baseline blocks (mean ± SD) = 6.6 ± 0.6 vs 5.0 ± 0.5; $Z = 2.5$; $P < 0.05$; $N = 8$). Arousal increased for activation blocks as compared to baseline blocks (score for activation vs baseline blocks (mean ± SD) = 6.6 ± 0.4 vs 4.6 ± 1.6; $Z = 2.4$; $P < 0.05$; $N = 8$). He reported the use of mental imagery of winter landscapes, engaging in snowboarding and social interaction as his strategy to increase the BOLD signal. During baseline blocks, he attended to the signal time-course without performing any specific task.

## fMRI data

### *On-line analysis and continuous feedback of BOLD time-course*

The implemented fMRI brain–computer interface (BCI) displayed a continuously updated BOLD time-course of the dorsal and the rostral–ventral anterior cingulate cortex (ACC) with a delay of less than 2 s from image acquisition. Fig. 2a and b shows screenshots of the display presented to the experimenter and to the subject, respectively.

### *Off-line analysis*

Head motions exhibited less than 0.6 mm translation and 0.8° rotation. In the first session only, changes of global signal intensity were correlated with the feedback task (descriptive $P < 0.001$).

### Region of interest analysis: dorsal and rostral–ventral subdivisions of ACC

ROI analysis revealed a significantly increased activity of dorsal ACC in five out of eight sessions during activation blocks ($P < 0.05$). In four sessions, the rostral–ventral ACC exhibited a significant increase of the BOLD signal ($P < 0.05$). Across all sessions, the effect of signal increase was highly significant for dorsal ACC ($P < 0.001$) and rostral–ventral ACC ($P < 0.01$). Table 1 lists the obtained signal changes during individual sessions. In addition, signal change of the rostral–ventral ACC increased with the number of the session indicating a potential learning effect ($r = 0.67$; $P < 0.05$; $N = 8$; see Fig. 4a). No significant correlations of the signal changes in regions of interest (ROIs) with behavioral measures, i.e., changes in arousal and emotional valence, were observed.

## Statistical parametric mapping

Significantly activated clusters are listed in Table 2. Locations of activations are given in MNI stereotaxic coordinates (Collins et al., 1994). Anatomical regions were labeled according to Tzourio-Mazoyer et al. (2002) and the ACC was divided into subdivisions as described previously.

Activations emerged in five brain regions: (1) rostral–ventral and dorsal ACC; (2) supplementary motor area (SMA); (3) gyrus rectus and frontal gyri; (4) superior anterior cerebellum; and (5) cuneus and calcarine fissure (Fig. 3a and Table 2). Two clusters of significant signal decreases were found in parietal and occipital cortex with their maxima at left superior parietal gyrus (MNI: [−36, −50, 60] mm; $t$ value 9.3; cluster size: 2239 voxels = 17.9 ml) and right precuneus (MNI: [10, −62, 56] mm; $t$ value 9.3; cluster size: 369 voxels = 3.0 ml).

To explore the presumptive learning effect yielded by the ROI analysis, we investigated whether the observed increase across sessions was specific for the rostral–ventral ACC. Each voxel of the imaged volume was tested for an increase of signal change across sessions (corrected $P < 0.01$, voxel and cluster level). Three clusters were found with maxima at the right hemispheric rostral–ventral ACC (MNI: [6, 34, 22] mm), the left hemispheric SMA (MNI: [−8, 16, 64] mm), and the left pallidum (MNI: [−8, 4, −2] mm).

## Discussion

We reported a technique to study physiological self-regulation of the BOLD-response using on-line feedback of the fMRI signal. Particular emphasis was placed on minimizing the delay between the feedback and the BOLD signal changes to facilitate self-regulation (e.g., Rockstroh et al., 1990) while performing standard data preprocessing.

Table 1
Activation of the dorsal and rostral–ventral anterior cingulate cortex (ACC), and the maximally activated voxel in the SMA during activation blocks

| Session number | Dorsal ACC | | Rostral–ventral ACC | | SMA (maximally activated voxel) | |
|---|---|---|---|---|---|---|
| | Signal change (%) | *t* value | Signal change (%) | *t* value | Signal change (%) | *t* value |
| 1 | **0.18** | **3.04** | −0.03 | −0.48 | 0.41 | 2.27 |
| 2 | −0.01 | −0.09 | 0.04 | 0.62 | 0.43 | 2.51 |
| 3 | 0.02 | 0.27 | −0.08 | −1.05 | 0.72 | 3.51 |
| 4 | **0.11** | **2.30** | **0.14** | **2.64** | 0.71 | 4.77 |
| 5 | 0.07 | 1.50 | 0.03 | 0.53 | 0.75 | 5.65 |
| 6 | **0.12** | **2.43** | **0.16** | **2.83** | 0.89 | 5.83 |
| 7 | **0.27** | **5.38** | **0.16** | **2.92** | 1.20 | 7.92 |
| 8 | **0.09** | **1.77** | **0.09** | **1.65** | 0.89 | 5.87 |
| Overall | **0.11** | **5.6** | **0.06** | **3.02** | 0.75 | 13.01 |

*Note.* Percent signal change per session measured from baseline and its level of significance (*t* value) are listed. Significant activations are set in boldface for regions of interest ($P < 0.05$). Note that the activation of the SMA is reported for the maximally activated voxel and not averaged across a region as in the case of the ACC.

To this end, a fMRI brain–computer interface (BCI) was developed based on real-time fMRI analysis (Goebel, 2001) which allowed to directly feed back the BOLD signal of specific brain regions, i.e., parts of the anterior cingulate cortex (ACC), with a maximum delay of 2 s from image acquisition to visual feedback.

We illustrated the concept of physiological self-regulation of BOLD-responses with exemplary data of one subject who was trained to control the BOLD signal of the rostral–ventral "affective" and dorsal "cognitive" subdivision of the ACC (Bush et al., 2000). The subject was able to significantly increase the signal of both subdivisions of the ACC during presentation of a discriminative stimulus. The achieved signal change in the "affective" subdivision of ACC (ACad) increased across the feedback sessions indicating a possible learning effect. The observed mean signal increase and its change across sessions was spatially not restricted to the ACC (cf. Figs. 3 and 4b). This generalization may be due to functional connectivity, e.g., between ACC and supplementary motor area (SMA), and the fact that the feedback signal did not provide information about activity in areas apart from the regions of interest. With this information coactivations might be suppressed by self-regulation.

Because it is well known that changes in the fMRI signal can be caused by artifacts and unspecific effects, such as head motion or cardiorespiratory effects, exceptional effort was applied to control them during acquisition and analysis of fMRI data. In order to reduce motion artifacts, motion correction was performed on-line. The estimated motion parameters were fed back to the subject who should keep them to a minimum. For off-line data analysis, first and second order motion parameters and spin history were included as covariates. This procedure suppressed residual motion artifacts after realignment (Friston et al., 1996).

The subject was breathing normally during the experiment, in order to avoid signal changes caused by cardiorespiratory effects, which have been reported for relatively extreme physiological states such as hypercapnia induced by at least 30 s breath holding or inhalation of $CO_2$-enriched air (Kastrup et al., 2001) and certain meditative states sustained for several minutes (Lazar et al., 2000). The global

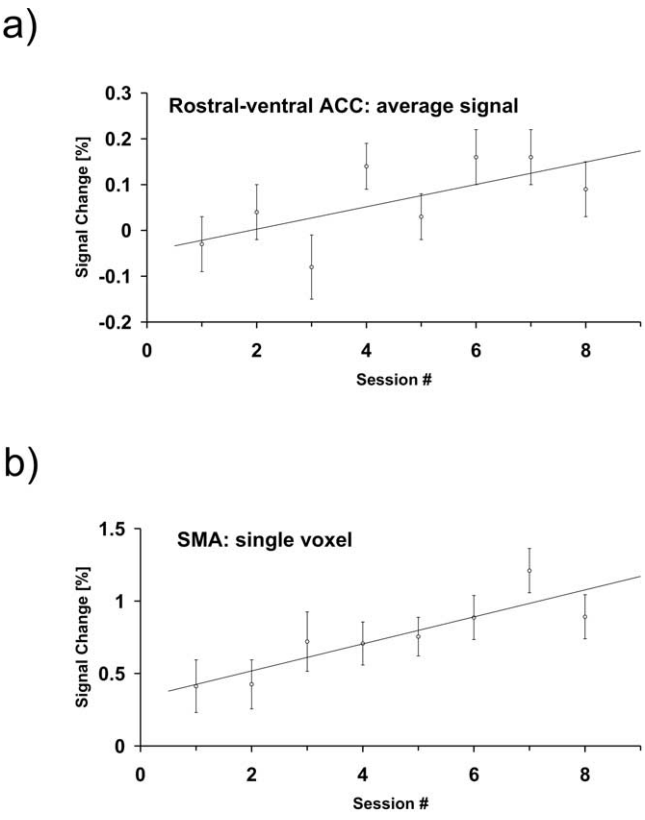


Fig. 4. Quantitative analysis across sessions. (a) The detected change in the *average* BOLD signal of the rostral–ventral anterior cingulate cortex (ACC) increased across feedback sessions suggesting a learning effect ($r = 0.67$, $P < 0.05$). (b) Comparable to the rostral–ventral ACC, the change in BOLD signal of the supplementary motor area (maximally activated voxel in SMA; MNI: [−2, 16, 52] mm) increased across sessions ($r = 0.95$, $P < 0.001$). It is not surprising that the presumptive learning effect did not only emerge in the rostral–ventral ACC, because the feedback signal did not provide information about the activity in other brain areas such as SMA. Note that graphs are scaled differently.

Table 2
Clusters of significant signal increase during activation blocks

| Region | MNI coordinates (mm) | Cluster size (voxel)/(ml) | *t* value |
|---|---|---|---|
| **L supplementary motor area** | **−2, 16, 52** | **2202/17.6** | **13.0** |
| L anterior cingulate cortex, dorsal subdivision | −10, 22, 26 | | 7.6 |
| L anterior cingulate cortex, dorsal subdivision | −2, 24, 30 | | 7.3 |
| **Cerebellar vermis III** | **0, −44, −10** | **2359/18.9** | **9.2** |
| L calcarine fissure | −12, −54, 4 | | 6.8 |
| L thalamus | −6, −32, 6 | | 6.6 |
| **R gyrus rectus** | **2, 48, −18** | **1631/13.0** | **8.1** |
| L middle frontal gyrus, orbital part | −2, 32, −14 | | 7.4 |
| R anterior cingulate cortex, rostral–ventral subdivision | 4, 26, −12 | | 7.1 |
| **L middle frontal gyrus** | **−34, 58, 14** | **394/3.2** | **7.3** |
| L superior frontal gyrus, dorsolateral part | −22, 64, 16 | | 6.3 |
| L superior frontal gyrus, dorsolateral part | −26, 66, 8 | | 6.3 |
| **L inferior frontal gyrus, orbital part** | **−32, 30, −6** | **197/1.6** | **7.2** |
| L middle frontal gyrus, orbital part | −28, 34, −18 | | 5.5 |
| **R calcarine fissure** | **4, −96, 6** | **531/4.2** | **7.1** |
| R cuneus | 4, −88, 18 | | 6.9 |
| L cuneus | −2, −100, 14 | | 6.6 |

*Note.* Most significant local maxima with a minimum separation of 8 mm exceeding the threshold of $P < 0.05$ (volume-corrected) within clusters of at least 100 voxels spatial extent. Location in left and right hemisphere is indicated by L and R, respectively. Bold numbers correspond to the highest peak of the cluster. Coordinates are given in MNI stereotaxic space (Collins et al., 1994) and labeled anatomically according to Tzourio-Mazoyer et al. (2002) and Devinsky et al. (1995).

signal intensity of the whole brain was not correlated with the feedback task, except for the first session, and statistical maps did not show global activation patterns, which would be expected in case of cardiorespiratory effects (Lazar et al., 2000; Kastrup et al., 2001).

The regional specificity of the physiological self-regulation might be improved by differential and bidirectional feedback tasks, e.g., increase of activity in the rostral–ventral ACC with simultaneous decrease of activity in the dorsal ACC or vice versa. Technical advances which allow a more precise definition of regions of interest on the cortical surface (Goebel, 2001) may further increase the specificity of the feedback training. In combination with optimized MR pulse sequences offering higher BOLD sensitivity (e.g., Posse et al., 2001; Mathiak et al., 2002) and insensitivity to susceptibility artifacts (e.g., Deichmann et al., 2002; Posse et al., 2003), brain areas such as the orbitofrontal cortex will be accessible to fMRI-feedback training as well.

The presented method promises to be a useful scientific tool to study the behavioral, cognitive, and emotional function of circumscribed brain areas. Behavior and cognition might be measured as a *dependent* variable of the locally regulated BOLD-response in addition to conventional neuroimaging studies which measure brain activity as a dependent variable of behavior or of sensory stimulation.

## Acknowledgments

This study was supported by the Deutsche Forschungsgemeinschaft (DFG, Bonn, Germany) SFB550/B5 and Bi 195/39, the WIN-Kolleg of the Heidelberg Academy of Sciences and Humanities (Germany), and the Federal Ministry of Education and Research (BMBF, Berlin, Germany). We thank B. Newport, B. Kardatzki, and F. Eippert for technical assistance. The authors thank S. Anders, H. Preissl, and K. Wiech for reading the manuscript and for helpful discussions.

## References

Arthurs, O.J., Boniface, S., 2002. How well do we understand the neural origins of the fMRI BOLD signal? Trends Neurosci. 25, 27–31.

Arthurs, O.J., Williams, E.J., Carpenter, T.A., Pickard, J.D., Boniface, S.J., 2000. Linear coupling between functional magnetic resonance imaging and evoked potential amplitude in human somatosensory cortex. Neuroscience 101, 803–806.

Ashburner, J., Friston, K.J., 1999. Nonlinear spatial normalization using basis functions. Hum. Brain Mapp. 7, 254–266.

Ball, T., Schreiber, A., Feige, B., Wagner, M., Lucking, C.H., Kristeva-Feige, R., 1999. The role of higher-order motor areas in voluntary movement as revealed by high-resolution EEG and fMRI. Neuroimage 10, 682–694.

Birbaumer, N., Elbert, T., Canavan, A., Rockstroh, B., 1990. Slow potentials of the cerebral cortex and behavior. Physiolog. Rev. 70, 1–41.

Birbaumer, N., Ghanayim, N., Hinterberger, T., Iversen, I., Kotchoubey, B., Kübler, A., Perelmouter, J., Taub, E., Flor, H., 1999. A spelling device for the paralysed. Nature 398, 297–298.

Bradley, M.M., Lang, P.J., 1994. Measuring emotion: the Self-Assessment Manikin and the Semantic Differential. J. Behav. Ther. Exp. Psychiatry 25, 49–59.

Brett, M., Christoff, K., Cusack, R., Lancaster, J., 2001. Using the Talairach atlas with the MNI template. Neuroimage 13, S85.

Bush, G., Luu, P., Posner, M.I., 2000. Cognitive and emotional influences in anterior cingulate cortex. Trends Cogn. Sci. 4, 215–222.

Collins, D.L., Neelin, P., Peters, T.M., Evans, A.C., 1994. Automatic 3D intersubject registration of MR volumetric data in standardized Talairach space. J. Comput. Assist. Tomogr. 18, 192–205.

Cox, R.W., Jesmanowicz, A., 1999. Real-time 3D image registration for functional MRI. Magn. Reson. Med. 42, 1014–1018.

Cox, R.W., Jesmanowicz, A., Hyde, J.S., 1995. Real-time functional magnetic resonance imaging. Magn. Reson. Med. 33, 230–236.

Critchley, H.D., Mathias, C.T., Dolan, R.J., 2001. Neuroanatomical basis for first- and second-order representations of bodily states. Nat. Neurosci. 4, 207–212.

Deichmann, R., Josephs, O., Hutton, C., Corfield, D.R., Turner, R., 2002. Compensation of susceptibility-induced BOLD sensitivity losses in echo-planar fMRI imaging. Neuroimage 15, 120–135.

Devinsky, O., Morrell, M.J., Vogt, B.A., 1995. Contributions of anterior cingulate cortex to behaviour. Brain 118, 279–306.

Eckstein, R., Collier-Brown, D., Kelly, P., 1999. Using Samba. O'Reilly, Cambridge.

Friston, K.J., Ashburner, J., Frith, C.D., Poline, J.-B., Heather, J.D., Williams, S.C., Frackowiack, R.S.J., 1995. Spatial registration and normalization of images. Hum. Brain Mapp. 2, 165–189.

Friston, K.J., Williams, S., Howard, R., Frackowiak, R.S., Turner, R., 1996. Movement-related effects in fMRI time-series. Magn. Reson. Med. 35, 346–355.

Gati, J.S., Menon, R.S., Rutt, B.K., 2000. Field strength dependence of functional MRI signals, in: Moonen, C.T.W., Bandettini, P.A. (Eds.), Functional MRI, Springer, Berlin, pp. 277–282.

Gembris, D., Taylor, J.G., Schor, S., Frings, W., Suter, D., Posse, S., 2000. Functional magnetic resonance imaging in real time (FIRE): sliding-window correlation analysis and reference-vector optimization. Magn. Reson. Med. 43, 259–268.

Gering, D.T., Weber, D.M., 1998. Intraoperative, real-time, functional MRI. J. Magn. Reson. Imaging 8, 254–257.

Goddard, N.H., Hood, G., Cohen, J.D., Eddy, W.F., Genovese, C.R., Noll, D.C., Nystrom, L.E., 1997. Online analysis of functional MRI datasets on parallel platforms. J. Supercomput. 11, 295–318.

Goebel, R., 2001. Cortex-based real-time fMRI. Neuroimage 13, S129.

Goodyear, B.G., Gati, J.S., Menon, R.S., 1997. The functional scout image: immediate mapping of cortical function at 4 tesla using receiver phase cycling. Magn. Reson. Med. 38, 183–186.

Kastrup, A., Kruger, G., Neumann-Haefelin, T., Moseley, M.E., 2001. Assessment of cerebrovascular reactivity with functional magnetic resonance imaging: comparison of CO2 and breath holding. Magn. Reson. Imaging 19, 13–20.

Klose, U., Erb, M., Wildgruber, D., Müller, E., Grodd, W., 1999. Improvement of the acquisition of a large amount of MR images on a conventional whole body system. Magn. Reson. Imaging 17, 471–474.

Kotchoubey, B., Strehl, U., Uhlmann, C., Holzapfel, S., König, M., Froscher, W., Blankenhorn, V., Birbaumer, N., 2001. Modification of slow cortical potentials in patients with refractory epilepsy: a controlled outcome study. Epilepsia 42, 406–416.

Lazar, S.W., Bush, G., Gollub, R.L., Fricchione, G.L., Khalsa, G., Benson, H., 2000. Functional brain mapping of the relaxation response and meditation. Neuroreport 11, 1581–1585.

Logothetis, N.K., Pauls, J., Augath, M., Trinath, T., Oeltermann, A., 2001. Neurophysiological investigation of the basis of the fMRI signal. Nature 412, 150–157.

Mathiak, K., Posse, S., 2001. Evaluation of motion and realignment for functional magnetic resonance imaging in real time. Magn. Reson. Med. 45, 167–171.

Mathiak, K., Rapp, A., Kircher, T.T.J., Grodd, W., Hertrich, I., Weiskopf, N., Lutzenberger, W., Ackermann, H., 2002. Mismatch responses to randomized gradient switching noise as reflected by fMRI and whole-head magnetoencephalography. Hum. Brain Mapp. 16, 190–195.

Mulholland, T., Boudrot, R., Davidson, A., 1979. Feedback delay and amplitude threshold and control of the occipital EEG. Biofeedback Self Regul. 4, 93–102.

Nowinski, W.L., Bryan, R.N., Raghavan, R., 1997. The Electronic Clinical Brain Atlas: Multiplanar Navigation of the Human Brain. Thieme, New York.

Paus, T., 2001. Primate anterior cingulate cortex: where motor control, drive and cognition interface. Nat. Rev. Neurosci. 2, 417–424.

Pollock, D.S.G., 1999. A Handbook of Time-Series Analysis, Signal Processing and Dynamics. Academic Press, San Diego, CA.

Posse, S., Binkofski, F., Schneider, F., Gembris, D., Frings, W., Habel, U., Salloum, J.B., Mathiak, K., Wiese, S., Kiselev, V., Graf, T., Elghahwagi, B., Grosse-Ruyken, M.L., Eickermann, T., 2001. A new approach to measure single-event related brain activity using real-time fMRI: feasibility of sensory, motor, and higher cognitive tasks. Hum. Brain Mapp. 12, 25–41.

Posse, S., Fitzgerald, D., Goo, K., Habel, U., Rosenberg, D., Moore, G.J., Schneider, F., 2003. Real-time fMRI of temporolimbic regions detects amygdala activation during single-trial self-induced sadness. NeuroImage 18, 760–768.

Rockstroh, B., Elbert, T., Birbaumer, N., Lutzenberger, W., 1990. Biofeedback-produced hemispheric asymmetry of slow cortical potentials and its behavioral effects. Int. J. Psychophysiol. 9, 151–165.

Rorden, C., Brett, M., 2000. Stereotaxic display of brain lesions. Behav. Neurol. 12, 191–200.

Smyser, C., Grabowski, T.J., Frank, R.J., Haller, J.W., Bolinger, L., 2001. Real-time multiple linear regression for fMRI supported by time-aware acquisition and processing. Magn. Reson. Med. 45, 289–298.

Tzourio-Mazoyer, N., Landeau, B., Papathanassiou, D., Crivello, F., Etard, O., Delcroix, N., Mazoyer, B., Joliot, M., 2002. Automated anatomical labeling of activations in SPM using a macroscopic anatomical parcellation of the MNI MRI single-subject brain. Neuroimage 15, 273–289.

Vogt, B.A., Nimchinsky, E.A., Vogt, L.J., Hof, P.R., 1995. Human cingulate cortex: surface features, flat maps, and cytoarchitecture. J. Comp. Neurol. 259, 490–506.

Voyvodic, J.T., 1999. Real-time fMRI paradigm control, physiology, and behavior combined with near real-time statistical analysis. Neuroimage 10, 91–106.

Worsley, K.J., Friston, K.J., 1995. Analysis of fMRI time-series revisited—again. Neuroimage 2, 173–181.

Worsley, K.J., Marrett, S., Neelin, P., Vandal, A.C., Friston, K.J., Evans, A.C., 1996. A unified statistical approach for determining significant voxels in images of cerebral activation. Hum. Brain Mapp. 4, 58–73.

Yoo, S.S., Jolesz, F.A., 2002. Functional MRI for neurofeedback: feasibility study on a hand motor task. Neuroreport 13, 1377–1381.